PERGAMON

Electrochimica Acta 45 (2000) 4449–4456

ELECTROCHIMICA Acta

www.elsevier.nl/locate/electacta

The bubble coverage of gas-evolving electrodes in a flowing electrolyte

J. Eigeldinger [1], H. Vogt *

TFH Berlin-University of Applied Sciences, Laboratory of Reaction Technology, D-13353 Berlin, Germany

Received 17 January 24456; received in revised form 27 March 2000

Abstract

During operation of gas-evolving electrodes, a fraction of the electrode surface is covered with adhering gas bubbles, which are known to exert substantial effect on mass and heat transfer, on overpotential, on limiting current density and on ohmic resistance. For this reason, many investigations were conducted to obtain experimental data of the fractional bubble coverage (or fractional shielding) in stagnant liquids. However, very little attention has been paid to the behaviour in liquid flow, although the majority of industrial electrochemical reactors are operated with flowing electrolyte liquids. The paper presents a theoretical analysis and experimental results of the effect of liquid velocity on the bubble coverage.

Keywords: Bubble coverage; Gas-evolving electrodes; Electrolyte flow

Nomenclature

A	electrode surface area (m^2)
$\bar{A}_b$	mean gas–liquid interface of bubble (m^2)
Δc	concentration difference at electrode surface (mol m^{-3})
Δc_b	concentration difference at bubble (mol m^{-3})
C_1	parameter, Eq. (24) (m^2)
C_2	parameter, Eq. (25) (s m^{-1})
C_3	constant, Eq. (26) (m^2)
C_4	constant, Eq. (27) (s m^{-1})
d	equivalent bubble diameter, Eq. (16) (m)
D	diffusion coefficient (m^2 s^{-1})
F	Faraday constant, $F = 96487$ A s mol^{-1}
f_G	gas evolution efficiency
F	force (kg m s^{-2})
g	acceleration due to gravity (m s^{-2})
H	bubble height (m)
I	current (A)

* Corresponding author. Fax: +49-30-45042008.

E-mail address: vogt@tfh-berlin.de (H. Vogt).

[1] Present address. Thielenhaus Microfinish Corp., 42925 W. Nine Mile Road, Novi, MI 48375, USA.

0013-4686/00/$ - see front matter

PII: S0013-4686(00)00513-2

j	true current density (A m^{-2})
k	mass transfer coefficient (m s^{-1})
k_b	mass transfer coefficient at gas–liquid interface (m s^{-1})
K_1	numerical constant, Eqs. (4a) and (4b)
K_2	numerical constant, Eq. (21)
M	molar mass (kg mol^{-1})
n	charge number
R	bubble radius (m)
R_0	radius of contact area (m)
R_m	universal gas constant, $R_m = 8.3143$ kg m^2 s^{-2} mol^{-1} K^{-1}
R_r	bubble radius on detachment (m)
t	time (s)
t_r	residence time (s)
v	flow velocity (m s^{-1})
$\bar{v}$	average flow velocity in channel (m s^{-1})
v^*	average flow velocity at adhering bubble (m s^{-1})
y	coordinate normal to main flow direction (m)
Y	channel width (m)
z	number of adhering bubbles
ε	current efficiency
γ	interfacial tension (kg s^{-2})
η	dynamic viscosity (kg m^{-1} s^{-1})
ϑ	contact angle
Θ	fractional bubble coverage of electrode surface
Θ_0	fractional bubble coverage at $v = 0$
υ	stoichiometric number
ρ	density (kg m^{-3})
ζ	drag number
Ja	Jakob number, Eq. (6)
Re_v	Reynolds number, Eq. (8)
Sc	Schmidt number, $Sc \equiv \eta_L/(\rho_L D)$
Sh_b	Sherwood number, Eq. (7)

Subscripts

G	gas
L	liquid
R	detachment

1. Introduction

Operation of electrodes without gas evolution differs from that of gas-evolving electrodes in that the electrochemical processes of the latter ones are superimposed by physical processes induced by gas bubbles adhering to the electrode. These bubbles not only deactivate the parts of the electrode surface that they cover or shield, but their growth also causes microflow in the electrode boundary layer. Both effects strongly interfere with the operation of the electrode.

It is known that the fraction of the electrode surface covered with or shielded by adhering bubbles is an important operation parameter. A degree of coverage (Bedeckungsgrad) was introduced by Ibl and Venczel in 1961 and defined as the fraction of the electrode surface contacted by adhering bubbles [1,2]. For non-wetting liquids or bubbles with contact angles $\vartheta \geq 90°$, this definition is unproblematic. Such contact angles occur in molten salts under certain conditions. Operating electrodes in contact with aqueous electrolyte solutions commonly exhibit contact angles close to zero. A more general definition for arbitrary values of the contact angle was given in 1980 [3]: The bubble coverage Θ denotes the fraction of the electrode area shaded by normal projection on the electrode surface, Fig. 1. Even from today's view-point this definition appears reasonable since the area below an adhering bubble essentially

does not participate in electrode reaction as shown by estimates of Tobias [4,5] and Müller [6] and their coworkers.

The action of bubbles adhering to the electrode surface is manifold. As the covered fraction of the electrode surface is electrochemically completely inactive, the true current density j of gas-evolving electrodes is larger than the nominal current density, I/A. As the current density below bubbles in wetting liquids, $\vartheta < 90°$, is very small [5,6] the true current density is approximately

$$j = \frac{I}{A}\frac{1}{1-\Theta} \tag{1}$$

Therefore, the adhering bubbles, represented by the fractional bubble coverage Θ, affect the slope of I-U curves and necessitate corrections of measured 'electrode overpotential' data or particular means to eliminate the detrimental action of bubbles [7].

For the same reason, Θ controls the upper operational limit given by the limiting current density. As seen from Eq. (1) the true current density may be substantially larger than at electrodes without gas evolution as the bubble coverage approaches unity. The limiting current density is reached at moderate values of the nominal current density if smooth gas release is impeded, e.g. at gas-evolving electrodes facing downwards. This fact is of particular importance in industrial alumina electrolysis, since it explains the action of the bubble coverage on the so-called anode effect [8,9].

Bubbles in the interelectrode gap are known to induce an increase in the ohmic interelectrode resistance. As the volumetric gas fraction is nowhere larger than in the bubble layer contacting the gas-evolving electrode [10] the bubble coverage Θ plays an important role and serves as a parameter to estimate ohmic voltage drop [11,12].

Finally, bubbles in contact with the electrode surface affect heat transfer and, particularly, mass transfer of reactant to and of product from the electrode surface in a more complex way. Adhering bubbles not only reduce the active area of heat and mass transfer but induce additional effect by the microconvection in the vicinity of the growing gas bubbles pushing away liquid in radial directions with large velocity. Furthermore, detaching bubbles cause turbulences in the electrode boundary layer enhancing heat and mass transfer [13]. Mass transfer equations are commonly written in the form

$$\frac{I\varepsilon}{(n/\upsilon)F} = kA\Delta c \tag{2}$$

not exhibiting the bubble coverage. This definition must not suggest that the bubble coverage is not involved. All available mass transfer equations [13] incorporate it in the mass transfer coefficient k. In case a mass transfer equation does not explicitly exhibit Θ [14] it is an approximation applicable in a limited range of the (nominal) current density where the shielding effect is fairly compensated by the action of microconvection.

In application to the gaseous product the situation is further complicated by the fact that the product is transported from the electrode by two possible paths [15,16]. The product, primarily formed at the electrode as dissolved gas is not totally transferred to the bulk; a fraction of the total rate is transferred to the gas–liquid interface of the adhering bubbles (or more strictly, of the bubbles present in the concentration boundary layer of the electrode), crosses the interface and causes bubble growth. Only the complementary amount enters the bulk. As a result, the mass flow rate to the bulk varies within the concentration boundary layer. Mass transfer equations for dissolved gas take this feature into account [17]. It stands to reason that the bubble coverage is the controlling parameter in that it affects not only the active electrode area and the (nearly congruent) mass transfer area but also the gas–liquid interfacial area and thus the effective rate of mass transfer to the bulk.

The value of the fractional bubble coverage Θ is not only affected by the conditions of mass transfer to adhering bubbles. Bubbles at electrodes can only be formed at active nucleation sites, i.e. irregularities on the electrode surface. Therefore, Θ depends on state and material of the electrode surface. Moreover, nucleation requires a sufficient interfacial supersaturation with dissolved gas which, in turn is controlled by the current density and the mass transfer coefficient k. The latter is affected by the above mentioned (bubble-induced) microconvection and also by (liquid flow-induced) macroconvection. In this way, the velocity of liquid flow parallel to the electrode surface must exert effect on the bubble coverage.

Hitherto, little notice has been taken of this effect. Numerous experimental data are available for stagnant electrolytes, but only one old, but valuable investigation on flowing liquids is known to the authors. Sillen [18,19] investigated the bubble coverage at anodes and

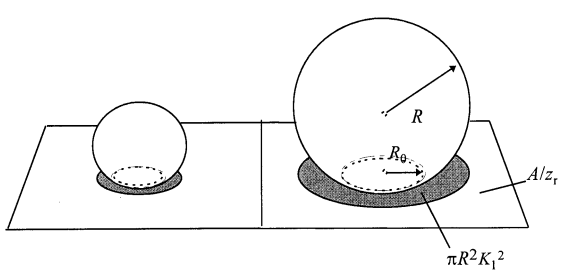

Fig. 1. Definition of the fractional bubble coverage.

cathodes in flowing KOH solution and presented some data showing the effect of current density and of flow velocity. Data of Θ decreased as the flow velocity was increased. Sillen concluded that the action on Θ is probably small at large values of the nominal current density and low velocity.

Usually, estimates of mass transfer or limiting current density are satisfied with bubble coverage data obtained in stagnant electrolyte, i.e. the common laboratory arrangement. However, this procedure would only be justified in case discrepancies to flowing liquids are not noticeable. As shown below, such simplification is not admissible if the velocity is not very small. Industrial electrochemical reactors are all (or at least in the vast majority of cases) operated with flowing electrolyte. Flow velocities in the order of 1 m s^{-1} are not extraordinary. It is the object of the present paper to develop a theoretical basis of the action of flow velocity on the fractional bubble coverage and to verify the result by laboratory investigation.

2. Theory

Since the area below an adhering bubbles with contact angles $\vartheta \leq 90°$ essentially does not participate in electrode reaction, the projected area is considered the covered area. The fractional bubble coverage of bubbles with arbitrary contact angles $0 \leq \vartheta \leq 180°$ may generally be described by [20]

$$\Theta \equiv \frac{z}{A\, t_r}\, K_1^2 \int_0^{t_r} \pi\, R^2\, \mathrm{d}t \tag{3}$$

where z denotes the number of bubbles simultaneously adhering to the electrode area A. t_r is the average residence time of bubbles with growing radius R.

$$K_1 = 1 \quad \text{for } \vartheta \leq 90° \tag{4a}$$

$$K_1 = \sin \vartheta \quad \text{for } \vartheta \geq 90° \tag{4b}$$

Growth of the bubble radius follows from a mass balance,

$$\frac{\mathrm{d}R}{\mathrm{d}t} = k_b\, Ja \tag{5}$$

where the Jakob number contains the supersaturation with dissolved gas

$$Ja \equiv \frac{M_G}{\rho_G}\, \Delta c_b = \frac{R_m\, T}{p}\, \Delta c_b \tag{6}$$

In flowing liquids, the law of bubble growth results from available mass transfer equations [21], for values of the Schmidt number typical of electrolyte solutions simplifying to

$$Sh_b \equiv \frac{k_b\, 2R}{D} = 2 + 0.79\ \mathrm{Re}_v^{0.5}\ Sc^{1/3} \tag{7}$$

where

$$\mathrm{Re}_v \equiv \frac{v^* 2R\rho_L}{\eta_L} \tag{8}$$

v^* denotes an average flow velocity at the adhering bubble. For the case of stagnant liquid, $v^* = 0$, combining Eqs. (5) and (6) gives after integration

$$R = (2Ja\, D\, t)^{0.5} \tag{9}$$

In channel flow, the local velocity $v = v(y)$ varies with the distance y from the electrode surface. At laminar flow the interrelation to the mean velocity $\bar{v}$ in an rectangular flow channel is

$$\frac{v}{\bar{v}} = 6\, \frac{y}{Y}\left(1 - \frac{y}{Y}\right) \tag{10}$$

where Y denotes the interpolar distance (or electrode-membrane distance). As the bubble diameter is small compared to the interpolar distance, Eq. (10) reduces to

$$\frac{v}{\bar{v}} \approx 6\, \frac{y}{Y} \tag{11}$$

At turbulent flow, the corresponding expression would approximately be

$$\frac{v}{\bar{v}} \approx 7.2\, \frac{y}{Y} \tag{12}$$

and is not very different from Eq. (11). With the bubble height $H = R(1 + \cos \vartheta)$ follows

$$v^* = \int_0^H v\, \frac{dy}{H} = 3\bar{v}\, \frac{R}{Y}\, (1 + \cos\, \vartheta) \tag{13}$$

and the bubble radius for the limiting case of very large flow velocities, $v \to \infty$.

$$R = 0.97\left[\frac{\bar{v}\, \rho_L}{Y\eta_L}\, (1 + \cos\, \vartheta)\right]^{0.5} Sc^{1/3} Ja\, Dt \tag{14}$$

A numerical check shows that discrepancies between Eqs. (9) and (14) are negligibly small for radii of bubbles at gas-evolving electrodes to result in the fractional bubble coverage

$$\Theta = \frac{\pi}{2}\, K_1^2 \left(\frac{R_r}{d}\right)^2 \frac{z}{A}\, d^2 \tag{15}$$

where R_r denotes the bubble radius immediately before detachment from the electrode or removal from the nucleation site in case of bubbles slipping along the electrode surface. The equivalent detachment diameter d, i.e. the diameter of a sphere with the volume of the bubble detaching from the nucleation site, follows from a geometrical consideration under assumption of a truncated sphere

$$\frac{d}{R_r} = [2(1 + \cos\, \vartheta)^2\, (2 - \cos\, \vartheta)]^{1/3} \tag{16}$$

Eq. (15) shows that the fractional bubble coverage mainly depends on two quantities: the break-off diameter d and the bubble population density z/A.

2.1. Detachment diameter and bubble population density

In stagnant liquid, the bubble detaches from the electrode, when the difference of gravitational force and buoyancy force exceeds the adhesion force. In flowing liquids the bubble is likely to detach from the surface when it moves from the nucleation site parallel to the electrode surface, coalesces with adhering bubbles or collides and is diverted from the surface. The process is the more facilitated the larger the sum of drag force and buoyancy force. Since the interfacial tension force parallel to the wall is then smaller than the adhesion force [22], it is reasonable to establish a balance formed of gravitational force, buoyancy force, drag force and interfacial tension force. The resolution of forces parallel to the wall was essentially successfully applied by Al-Hayes and Winterton [22] to gas bubbles detaching from electroneutral surfaces. Evaluation of experimental data have shown that further forces such as inertial force, force due to internal circulation and excess pressure force, although active, are insignificant [23].

The shape of adhering bubbles is approximated by that of truncated spheres with radius R and contact angle ϑ. The difference of gravitational force and buoyancy force of an adhering gas bubble is

$$F_1 = \frac{4}{3}\,\pi R^3 g(\rho_L - \rho_G)\frac{(1+\cos\ \vartheta)^2\,(2-\cos\ \vartheta)}{4} \tag{17}$$

The drag force exerted by the flow of liquid past the electrode surface to an adhering bubble idealised as a truncated sphere is [22]

$$F_2 = \zeta\rho_L\frac{v^{*2}}{2}\ \pi R^2\left(1-\frac{\vartheta-\cos\ \vartheta\ \sin\ \vartheta}{\pi}\right) \tag{18}$$

The drag number ζ generally depends on the Reynolds number, Eq. (8), and, for bubbles adhering to a wall, on the distance of neighbouring bubbles. A satisfactory correlation of theoretical [21] and experimental data [24] after introduction of the bubble coverage Θ, restricted to small Reynolds numbers is

$$\zeta = \frac{20}{\mathrm{Re}}\left(\frac{1}{1+\sqrt{\Theta}}\right) \tag{19}$$

The drag force under consideration of Eq. (11) results in

$$F_2 = \frac{15\,\pi\,R^2\,\eta_L\,\bar{v}}{Y}\left(\frac{1}{1+\sqrt{\Theta}}\right)(1+\cos\ \vartheta)\left(1-\frac{\vartheta-\cos\ \vartheta\ \sin\ \vartheta}{\pi}\right) \tag{20}$$

The interfacial tension force parallel to the electrode surface depends on the difference of the receding angle ϑ_r and the advancing angle ϑ_a on the circumference of the line of three-phase equilibrium, $2\pi R_0$. Since the contact angle varies on the line of contact, an average of local values must be used [25], here taken into account by a multiplier K_2.

$$F_3 = 2\pi R_0\,\gamma(\cos\ \vartheta_r - \cos\ \vartheta_a)K_2 = 2\pi R\,\sin\ \vartheta\,\gamma(\cos\ \vartheta_r - \cos\ \vartheta_a)K_2 \tag{21}$$

Winterton [26] proposed a multiplier $K_2 = 0.25$ later extended by a term strongly dependent on the mean contact angle [22].

From the balance of forces on detachment from the nucleation site

$$F_1 + F_2 - F_3 = 0 \tag{22}$$

follows with $R = R_r$ and under consideration of Eq. (16)

$$d = \sqrt{C_1}\left[\sqrt{1+\left(\frac{C_2\bar{v}}{1+\sqrt{\Theta}}\right)^2} - \frac{C_2\bar{v}}{1+\sqrt{\Theta}}\right] \tag{23}$$

with the abbreviations

$$C_1 \equiv 12\,\frac{R_r}{d}\,\frac{\gamma}{g(\rho_L-\rho_G)}\ \sin\ \vartheta\ (\cos\ \vartheta_r - \cos\ \vartheta_a)K_2 \tag{24}$$

$$C_2 = \frac{45}{\sqrt{C_1}}\,\frac{\eta_L}{Yg(\rho_L-\rho_G)}\left(\frac{R_r}{d}\right)^2(1+\cos\ \vartheta)\left(1-\frac{\vartheta-\cos\ \vartheta\ \sin\ \vartheta}{\pi}\right) \tag{25}$$

The diameter d is seen to decrease as the flow velocity is increased in agreement with experimental results of Winterton [23]. The finding is also in qualitative agreement with results obtained under conditions of electrochemical machining [27], although referring only to freely moving bubbles after detachment from the electrode.

The second unknown term in Eq. (15), the bubble population density z/A, depends on the supersaturation with dissolved gas affecting the activation of nucleation sites and, hence, on the current density. The surface density of nucleation sites depends on surface condition and material of the electrode. Owing to the complexity of the problem, a reliable prediction of the bubble population density is not possible at present. However, our experimental results in agreement with findings by Sillen [18] show that the bubble population density decreases with increasing flow velocity, tentatively to be expressed by

$$\frac{z}{A} = \frac{\Theta^{0,5}}{C_3} \tag{26}$$

as seen from Fig. 2. C_3 takes account of current density, surface condition and material.

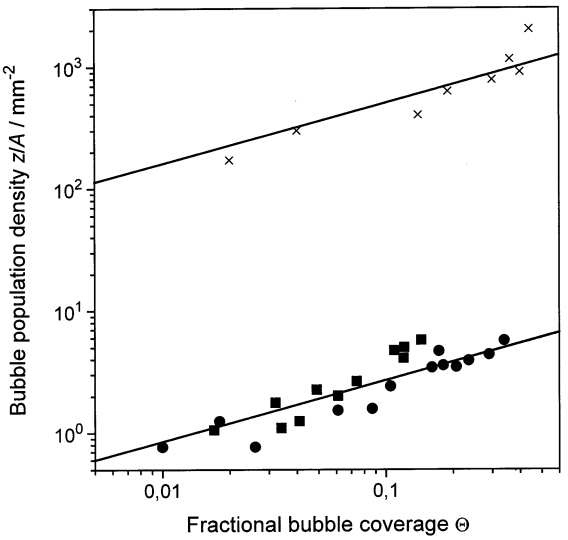

Fig. 2. Bubble population density vs. fractional bubble coverage. Graphite cathode: ■ — $I/A = 21$ A m^{-2}; ● — 104 A m^{-2}. For comparison nickel cathode: × — 2000 A m^{-2} from Sillen [19].

2.2. Fractional bubble coverage

For practical application an empirical relationship is proposed taking account of the facts that the force induced by the flow velocity increases with the square of the velocity and that the bubble coverage in stagnant liquid coincides with the value Θ_0 for $\bar{v} = 0$.

$$\Theta = \frac{\Theta_0}{[1 + (C_4\bar{v})^2]^2} \tag{27}$$

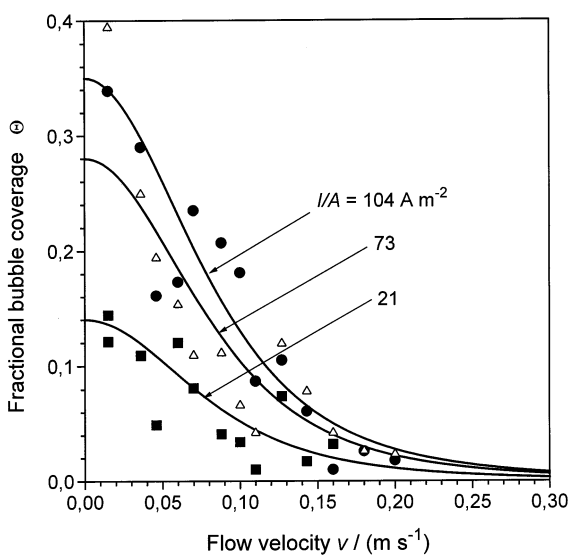

Fig. 3. Effect of flow velocity on fractional bubble coverage. Graphite cathode. ■ — $I/A = 21$ A m^{-2}; △ — 73 A m^{-2}; ● — 104 A m^{-2}.

Θ_0 depends on the current density and the surface condition of the electrode surface, and C_4 is an empirical parameter, which is constant at least for a given system.

3. Experimental

Experiments were conducted at hydrogen-evolving electrodes of various materials-copper, stainless steel, graphite-in 1 M KOH solution of 25°C and atmospheric pressure and flow velocities in the range of 0.02–0.25 m s^{-1}. Flow direction was parallel to the electrode surface.

The experimental set-up consisted of a pump-circulation system with a slightly inclined rectangular flow channel with a cross-sectional area of 19 mm × 52 mm. The circular working electrode of 35 mm diameter was embedded in the bottom of the channel at a position equal to 26 hydraulic diameters from the liquid entrance to ensure essentially developed flow profile. The counter-electrode was positioned 12 mm above the working electrode and had a horse-shoe shape to allow for observing the working electrode from the top by a video camera. Cathodic nominal current densities were 21, 73 and 104 A m^{-2}. Prior to each set of recordings the electrodes were prepolarized.

The optical set-up was able to record the bubble population and the diameter of adhering bubbles in a visual field of 4.65 mm × 4.65 mm in sloping light. Reflexes arising from scratches, pits and other irregularities of the electrode surface which might have been confused with small adhering bubbles were eliminated by using pairs of shots of the same field and under the same conditions, but one showing the area with adhering bubbles under operating current and the other one without current applied and bubbles swept off. Through digital technique one of the shots was subtracted from the other one of the pair. The result was a view of exclusively the adhering bubbles. Applying an appropriate software [28] and setting a reasonable contrast value enabled a transformation of the data into values of the area to determine the fractional bubble coverage.

4. Results and discussion

Experimental results for various electrode materials and current densities are shown in Figs. 3–5 correlated by Eq. (27). The quantities Θ_0 and C_4 have been selected for best data fit. Θ_0 is known to depend strongly on current density, material and surface condition of the electrode. An approximate relationship for estimating Θ_0 was proposed previously [29]. The quan-

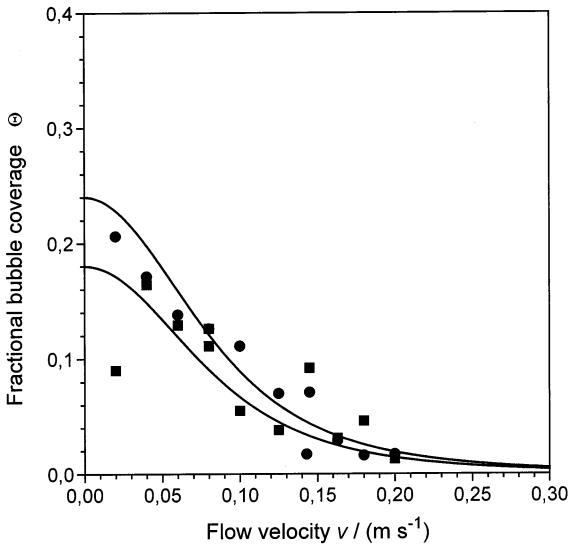

Fig. 4. Effect of flow velocity on fractional bubble coverage. Copper cathode. ■ — $I/A = 21$ A m^{-2}; ● — 104 A m^{-2}.

tity C_4 could generally be set $C_4 = 8$ s m^{-1} for all current densities and electrode materials.

The scatter of the experimental data points is seen to be substantial reflecting not only the numerous experimental uncertainties but also the fact that the bubble behaviour is of stochastic character which is the more pronounced the smaller the observed electrode partial area. Furthermore, it must be taken into consideration that the microprocesses are time-dependent and this effect may be strong in small partial areas. For these reasons, all results are charged with substantial uncertainties. However they show distinctly the strong decrease in the bubble coverage as the flow velocity increases to values common in industrial reactors. This result points out an important phenomenon not sufficiently taken notice of.

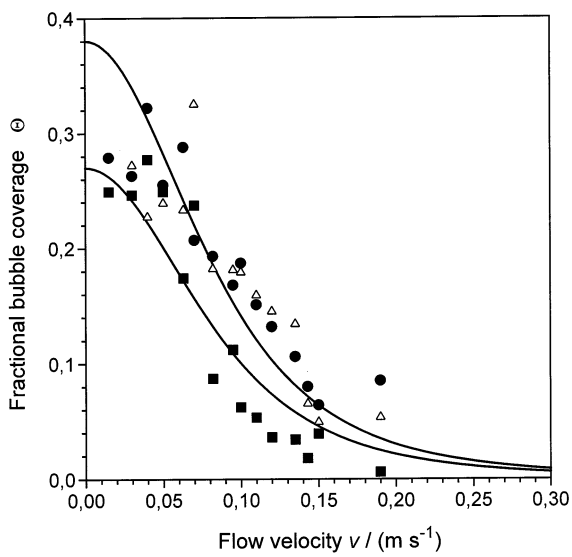

Fig. 5. Effect of flow velocity on fractional bubble coverage. Stainless steel cathode. ■ — $I/A = 21$ A m^{-2}; △ — 73 A m^{-2}; ● — 104 A m^{-2}.

Eq. (23) shows that the break-off diameter is substantially affected by the flow velocity. The finding is in agreement with the data of Sillen [18].

The extrapolated values of Θ_0 in Figs. 3–5 are larger than those published by other workers. The reason may be that the use of analysis programs in the present work provides a higher level of accuracy compared to other rather subjective and time-consuming procedures. Another, perhaps the main reason may be that the Θ_0 values refer to completely static liquid which in reality is not the case even in stagnant liquids where microconvective flow due to bubble growth and natural convection due to concentration gradients exist [30].

Sillen [18] proposed to distinguish subregions with different character at various flow velocities deduced from seemingly abrupt changes of slope in logarithmic $\Theta - v$ graphs. Such distinctly limited regions cannot be derived from the above theoretical consideration and should be doubted.

5. Conclusions

Liquid flow past the electrode surface strongly affects the fractional bubble coverage. Increasing velocity lowers the bubble coverage. Even moderate velocities, which are lower than flow velocities applied to many industrial reactors, reduce the bubble coverage substantially. At a velocity of about 0.3 m s^{-1} the bubble coverage is only a few percent of that in stagnant electrolyte.

This fact is notable in that ohmic interelectrode resistance, electrode overpotential and mass transfer to and from the electrode and, furthermore, the limiting current density are affected. Data of the fractional bubble coverage commonly obtained in experimental arrangements with stagnant electrolyte are not applicable to industrial reactors with liquid flow.

Microconvection induced by bubbles is widely considered to exert the controlling action on mass transfer at gas-evolving electrodes. But this view applies only to certain operation conditions. In stagnant liquid, free convection was shown to control mass transfer at low values of the current density. In flowing liquids, macroconvection not only superimposes other mass transfer mechanisms but is also seen to interfere with microconvective mass transfer by reducing the bubble coverage substantially.

References

[1] J. Venczel, Dissertation, Thesis, Swiss Federal Institute of Technology, Zurich, 1961.
[2] J. Venczel, Electrochim. Acta 15 (1970) 1909.
[3] H. Vogt, Electrochim. Acta 25 (1980) 527.
[4] P.J. Sides, C.W. Tobias, J. Electrochem. Soc. 127 (1980) 288.
[5] J. Dukovic, C.W. Tobias, J. Electrochem. Soc. 134 (1987) 331.
[6] M. Krenz, L. Müller, A. Pomp, Electrochim. Acta 31 (1988) 723.
[7] B. Kabanov, Acta Physicochim. USSR 5 (1936) 193.
[8] H. Vogt, J. Appl. Electrochem. 29 (1999) 137.
[9] H. Vogt, J. Appl. Electrochem. 29 (1999) 779.
[10] H. Riegel, J. Mitrovic, K. Stephan, J. Appl. Electrochem. 28 (1998) 10.
[11] P.J. Sides, C.W. Tobias, J. Electrochem. Soc. 129 (1982) 2715.
[12] H. Vogt, J. Appl. Electrochem. 13 (1983) 87.
[13] H. Vogt, Gas-evolving electrides, in: E. Yeager, J.O'M. Bockris, B.E. Conway, S. Sarangapani (Eds.), Comprehensive Treatise of Electrochemistry, vol. 6, Plenum, New York, 1983, pp. 455–489
[14] K. Stephan, H. Vogt, Electrochim. Acta 24 (1979) 11.
[15] H. Vogt, Electrochim. Acta 29 (1984) 167.
[16] F. Beck, H. Goldacker, G. Kreysa, H. Vogt, H. Wendt, Electrochemistry. In: Ullmann's Encyclopedia of Industrial Chemistry. Sixth Edition, 1998 Electronic Release, Wiley-VCH, Weinheim, 1998.
[17] H. Vogt, J. Appl. Electrochem. 19 (1989) 713.
[18] C.W.M.P. Sillen, Thesis Tech. Hogeschool Eindhoven 1983, pp. 45, 78.
[19] L.J.J. Janssen, C.W.M.P. Sillen, E. Barendrecht, S.J.D. van Stralen, Electrochim. Acta 29 (1984) 633.
[20] H. Vogt, Electrochim. Acta 42 (1997) 2695.
[21] H. Brauer, D. Mewes, Chemie-Ing.-Technik 44 (1972) 865.
[22] R.A.M. Al-Hayes, R.H.S. Winterton, Int. J. Heat Mass Transfer 24 (1981) 223.
[23] R.H.S. Winterton, Int. J. Heat Mass Transfer 27 (1984) 1422.
[24] A.J. Goldman, R.G. Cox, H. Brenner, Chem. Engng. Sci. 21 (1966) 1151.
[25] J.L. von Eichborn, Werkstoffe Korrosion 2 (1951) 212.
[26] R.H.S. Winterton, Chem. Engng. Sci. 27 (1972) 1223.
[27] D. Landolt, R. Acosta, R.H. Muller, C.W. Tobias, J. Electrochem.Soc. 117 (1970) 839.
[28] H. Bässmann, P.W. Besslich, Bildverarbeitung Ad Oculos, Springer, Berlin, 1993.
[29] H. Vogt, J. Electrochem. Soc. 137 (1990) 1179.
[30] H. Vogt, Electrochim. Acta 38 (1993) 1421.